

UC Riverside

UCR Honors Capstones 2021-2022

Title

Cytocompatibility of nanocrystalline yttria-stabilized zirconia ceramics for cranial window applications

Permalink

<https://escholarship.org/uc/item/2t83t151>

Author

Hung, Chengi

Publication Date

2022-06-01

Data Availability

The data associated with this publication are not available for this reason: N/A

Cytocompatibility of nanocrystalline yttria-stabilized zirconia ceramics for cranial window applications

By

Chengi Hung

A capstone project submitted for Graduation with University Honors

June, 2022

University Honors

University of California, Riverside

APPROVED

Dr. Huinan Liu

Department of Bioengineering

Dr. Richard Cardullo, Howard H Hays Jr. Chair

University Honors

ABSTRACT

Transparent yttria-stabilized zirconia (YSZ) ceramics are promising candidates for cranial window applications due to their excellent mechanical properties, optical transparency, and biocompatibility. Opposed to most widely known polymeric materials for artificial bone cement such as Poly-Lactic-co-Glycolic Acid (PLGA), Poly-Methyl Methacrylate (PMMA), and Polydimethylsiloxane (PDMS), YSZ ceramics offered tougher mechanical properties and better optical transparency. YSZ ceramics with different yttria contents had been reported to have great biocompatibility [1]. However, the cytocompatibility of YSZ ceramics with bone marrow-derived mesenchymal stem cells (BMSCs) is still lack of research. Here, we compared the YSZ disk processed via current-activated pressure-assisted densification (CAPAD) using commercial nanoparticle with 3, 6 and 8 mole percent of yttria (3YSZ, 6YSZ, 8YSZ), and YSZ densified via spark plasma sintering (SPS) using aerosol spray pyrolysis-synthesized nanoparticle with 4 and 8 mole percent of yttria (4YSZ_P and 8YSZ_P). The unpolished counterparts were labeled with an R, rough, at the end of the abbreviation of each fabrication method, for example 3YSZ_R. This study shows the unpolished YSZ discs had smaller spreading area than their polished counterparts with the same composition, no significant differences between the aspect ratio of BMSCs among different groups. The groups of 8YSZ, 8YSZ_R, 4YSZ_P, 4YSZ_PR, 8YSZ_P, and 8YSZ_PR were found to have the lower average cell adhesion densities than other YSZ ceramic groups under direct contact conditions. All the YSZ disc groups have similar cell adhesion densities to the Cell-only control. This study provides critical results to screen composition, processing, microstructure, and cytocompatibility of YSZ discs and establish their correlations for a potential candidate toward the transparent cranial window applications. This

study builds the foundation for future pre-clinical studies and clinical translation of YSZ implants

ACKNOWLEDGEMENTS

I would like to give a special thanks to Professor Huinan Liu and PhD candidate Changlu Xu. Their patience, assistance and support guided me to accomplish this capstone project under this difficult time. Since Professor Huinan Liu accepted my participation in her research group in my freshman year, I was surprised by how friendly and the eagerness to provide support for undergraduates. I want to say thank you again to Changlu, who guided me to here from zero knowledge in material science. I really enjoyed and appreciated these four years of support and encouragement. In addition, the results of this project paper have been accepted for publication in ACS applied biomaterials.

TABLE OF CONTENTS

1. Introduction	5
1.1 Brain injuries and diseases and light-based therapeutic solution	5
1.2 Materials for cranial implants	6
1.2.1 Polymeric Materials	6
1.2.2 Metallic Materials	7
1.2.3 Ceramic Materials	7
1.3 Materials for cranial window applications.....	7
2. Method	8
2.1 Preparation of YSZ samples	8
2.2 Evaluate cytocompatibility of YSZ samples in direct culture on BMSCs	9
3. Results	11
4. Discussion.....	18
5. Conclusion.....	20
6. Reference	21

1. Introduction

1.1 Brain injuries and diseases and light-based therapeutic solution

More people are suffering from traumatic brain injuries and brain diseases such as Parkinson's, Alzheimer's diseases, and traumatic brain injuries. For traumatic brain injuries, skulls are usually damaged and required treatments. Diagnosis, treatment, and medical care for patients with brain diseases, are burdensome for both the patients and the doctors because of the need of constant monitoring. In order to cure traumatic brain injuries, an artificial material is required to replace the defects. The materials chosen to replicate human skulls have to have similar mechanical strengths, biocompatibility and chemical properties between the skull and the brain tissues. The fabrication process and the price of the material also must be considered because the material must be able to precisely fabricate as the defects in a low cost. For brain diseases, there are still many diseases that are still untreatable due to lack of study, such as Alzheimer disease, Huntington disease, and Parkinson disease. The population who suffers from these diseases are relatively low, which leads to diminished economic value and hence results in an impedance in studies. To cure both traumatic brain injuries and brain diseases, craniotomies, open skull surgeries, are required. Especially studying and research brain diseases, repeated open skull surgeries are needed. The brain and blood flow have to be constantly monitored and provided treatment for a long period of time. Hence, repeated open skull surgeries highly increase the burden for the patients and greatly increase the price.

Recent decades, light based therapeutic solution had been introduced to treat brain diseases and injuries. For example, photo biomodulation therapy [2] utilized near-infrared light to cure from neurological to psychological conditions and photodynamic therapy utilized laser to

destroy gliomas and metastatic brain tumors and cancer. However, the poor penetration depth of light therapy resulted from the static and dynamic effects of optical scattering and absorption by the skull and tissues limited the potential and clinical usage of these light-based treatment. To address this challenge, cranial windows based on different materials such as polydimethylsiloxane (PDMS), glass, and nanocrystalline yttria-stabilized zirconia (YSZ) ceramic have been designed and studied. The cranial windows provide both protection and repeated optical access to the brain over a long term to meet the clinical needs of brain diagnosis and treatment.

1.2 Materials for cranial implants

Many materials had been introduced for treating brain diseases. The three main materials are polymeric, metallic, and ceramic materials.

1.2.1 Polymeric Materials

The advantages of polymeric materials are their excellence in biocompatibility with brain tissues, optical transparency of getting precise pictures on MRI and CT scans, and well-studied biodegradability respect with time and concentration of the materials. It is simple to mix polymeric materials with other materials such as hydroxyapatite that can improve bone rehabilitation. They are also easy to fabricate in complex shapes, such as scaffolding structure for guided bone regeneration. In addition, polymeric cranial implants eliminate the need of post-operation of removing because of their well-studied biodegradability. However, their major disadvantages are the weak mechanical property compared to that of the skull. Polymeric are usually the best for bone healing and guided bone regeneration [3][4], but they are just not strong enough to be sufficient in skull replacement. Furthermore, polymeric materials will be easily

penetrated by the laser therapy. Therefore, the use of polymeric materials in cranial implant is excluded.

1.2.2 Metallic Materials

In modern neurosurgical construction of cranial defects, titanium-based and titanium meshed combined with PMMA are most widely used. The advantages of metallic materials are their durability, resistance to corrosion friction and strong mechanical properties. However, their major disadvantages are also the inertness of biocompatibility, mechanical properties differences that may damage the brain tissues, and being too tough for the skull. [5] Furthermore, metallic material mixed with PMMA usually required replacement after 9years. [6] Metallic materials are still a sufficient material for open skull surgeries, but due to the lack of optical transparency which leads to incapability for light therapy, they are excluded.

1.2.3 Ceramic Materials

In modern joint surgical such as total hip replacement, total knee replacement, and total shoulder replacement, ceramic materials are always the best choice. The advantages of ceramics materials are their enhancement in lubrication, bone healing, especially hydroxyapatite, mechanical properties that are similar to skull, biocompatibility, and excellent resistance to corrosion and friction. [7][8] However, similar to metallic materials, they also lack ductility which suppress bone growth and healing. In contrast to the extreme toughness of metallic material, ceramic materials are similar to human skulls.

1.3 Materials for cranial window applications

Window to the brain applications is implanting a transparent material to the skull which create a “window” for monitoring and delivering treatments. Most importantly, this eliminate the needs of repeated open skull surgeries, which greatly alleviates the burden of patients and enhance

the convenience for the surgeons. Among the materials explored for the cranial window applications, polymers such as polydimethylsiloxane (PDMS) has the low compressive modulus of $< 0.75\text{-}2.08$ MPa, which is significantly lower than that of embalmed calvarium with a compressive modulus of $2.41\text{-}5.58$ GPa. PDMS windows thus provide limited protection to the brain. Glass has excellent transparency, but its brittleness limits its application as a cranial window. The YSZ ceramics, in contrast, have shown satisfying mechanical toughness and strength, good transparency, and excellent biocompatibility as a protective window to the brain.

Yttria stabilized zirconia (YSZ) is a strong ceramic material for cranial implant because of its potentials in the window to the brain applications. [9, 10] The optical transparency, optical access using infrared and different wavelengths laser, cerebral blood flow imaging, and mechanical properties of YSZ had been researched [7-9]. YSZ stands out to be a window to the brain materials based on its similar mechanical property to the human skull, precise optical access as serving a window to the brain and easy to fabricate. However, its response to cells has not yet been conducted and studied. In this research, we will experimentally determine the cytocompatibility of YSZ by direct culturing bone marrow mesenchymal stem cells (BMSCs) on different concentration and polished/unpolished YSZ samples and find out the best YSZ samples to the cytocompatibility of the BMSCs.

2. Method

2.1 Preparation of YSZ samples

Two different types of YSZ samples were provided by Dr. Garay's lab and Dr. Mangellini's lab. One YSZ samples were sintered using commercial nanoparticles and the other were sintered using spray pyrolysis-synthesized nanoparticles. The nanocrystalline YSZ samples were doped with 3, 6 and 8 mol.% yttria oxide (Y_2O_3) in the zirconia oxide (ZrO_2). These

samples will then be polished by using 30-micron diamond slurry on an automatic polisher and then polished using progressively finer abrasives from 30 μm to 1 μm . This polishing process not only would help us test the cytocompatibility of YSZ, but also increase the transparency of the samples. The polished YSZ samples sintered using commercial nanoparticles and ceramic sintering were named 3YSZ, 6YSZ and 8YSZ, and 3YSZ_np, 6YSZ_np, and 8YSZ_np respectively. Their unpolished counterparts were named as 3YSZ_R, 6YSZ_R and 8YSZ_R. The polished YSZ samples sintered via spray pyrolysis-synthesized nanoparticles via spark plasma sintering were named as 4YSZ_P and 8YSZ_P, and similarly the unpolished counterparts were named as 4YSZ_PR and 8YSZ_PR.

2.2 Evaluate cytocompatibility of YSZ samples in direct culture on BMSCs

Rat BMSCs were harvested and cultured following the approval by the Institutional Animal Care and Use Committee (IACUC) at the University of California at Riverside (UCR).

1.3 Evaluate cytocompatibility of YSZ samples in direct culture on BMSCs

A direct exposure culturing of YSZ had been conducted before [13]. However, in direct exposure culturing method, the surface roughness, surface free energy, hydrophilicity, protein deposition and the interaction between the surface of the YSZ to the BMSCs are unknown. Therefore, a direct culturing method is needed to analyze these properties.

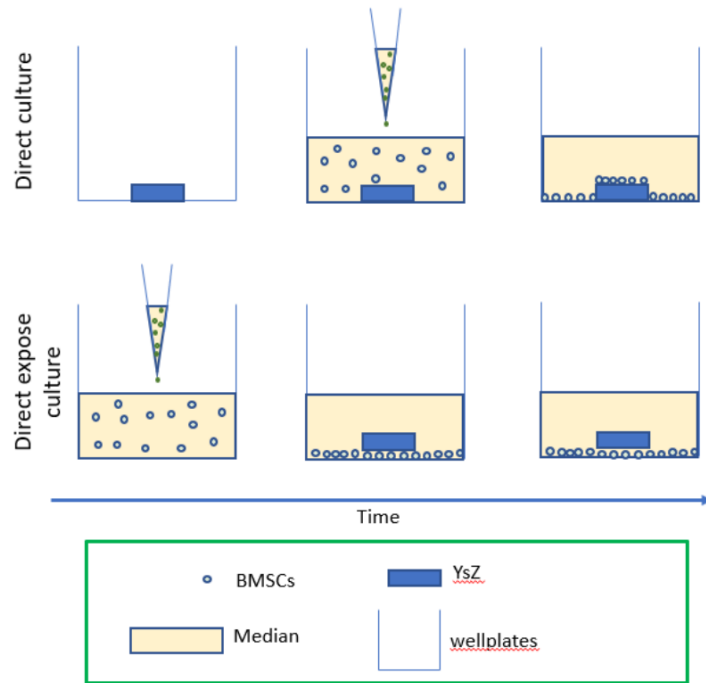


Figure 1. Direct Culturing

The YSZ ceramics sintered using commercial nanoparticles were cut into a diameter of 10mm. The volume and the mass were kept constant. The YSZ ceramics were also sterilized and dehydrated prior of direct culturing. Titanium disc and glass slide were used as control group. A standard 12-well tissue culture treated plated were used. The plates were first rinsed with Phosphate Buffered Saline (PBS) and Dulbecco's Modified Eagle Medium (DMEM) to calibrate the osmotic pressure under sterile conditions. Then the sterilized YSZ ceramics were placed in the culture wells. BMSCs were then cultured by directing seeding on top of the samples. BMSCs were harvested under standard cell culture conditions after 24 hours.

After harvesting, BMSCs attached on the YSZ ceramics in the well plates were fixed with 4% formaldehyde for 20 minutes. Then BMSCs were stained with Alexa Fluor 488-phalloidin (AF) for 20 minutes and 4',6-diamidino-2-phenylindole dilactate (DAPI) for 10minuts. AF stains the BMSCs actin to a bright green-fluorescent color and DAPI stains the nucleus to a blue color.

Then, the fluorescent results will be pictured using fluorescence microscope. The images will

finally be analyzed by ImageJ software to calculate cell spreading area, aspect ratio, and the number of cells for each different sample of YSZ ceramics.

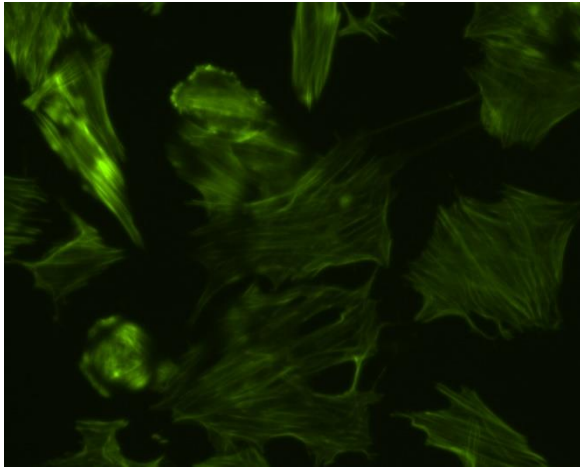


Figure 2. AF stain

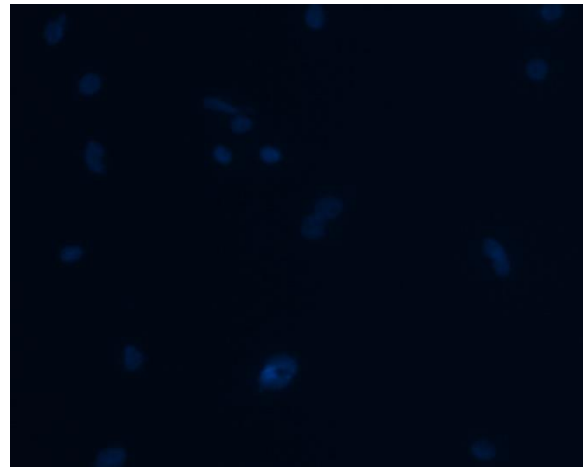


Figure 3. DAPI stain

3. Results

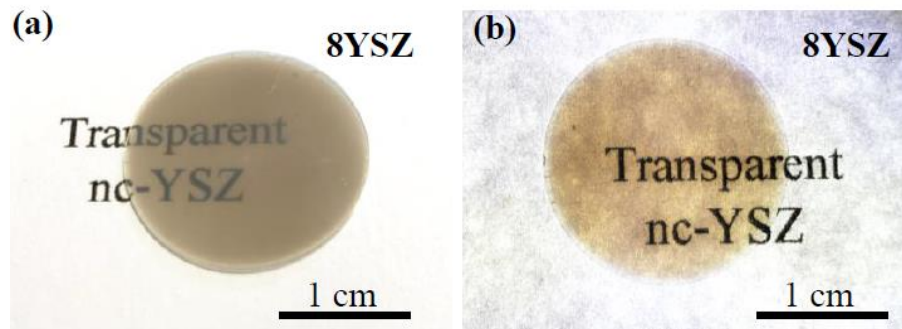


Figure 4. YSZ ceramics transparency

Figure 4 shows the YSZ ceramic transparency while placing the YSZ ceramic on top of a paper printed a line “Transparent nc-YSZ.” Figure 4a portrayed the light shined from above the sample, and 4b portrayed the light shined behind the paper. This figure demonstrated the transparency of YSZ, and its capabilities as window to the brain material.

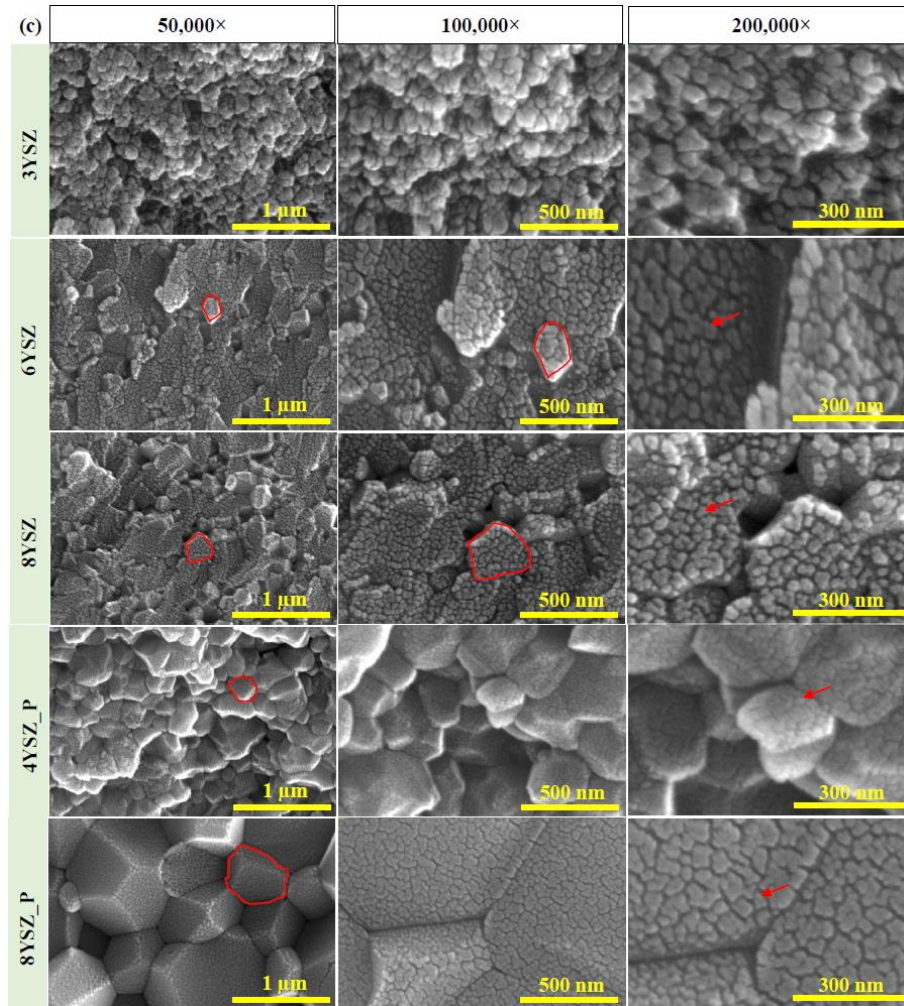


Figure 5. SEM Image of YSZ ceramic samples

Figure 5 shows the cross-sectional YSZ ceramic samples images under 50,000x, 100,000x, and 200,000x magnification taken by scanning electronic microscopy (SEM). The red circle indicates the large polycrystalline grains, and the red arrow shows the crystallite domains that composed the large polycrystalline grains. From the figure, we can see both the size of polycrystalline grains and crystallite domain decreases as the concentration of yttria increases. In addition, YSZ ceramics fabricated via commercial nanoparticles sintering were also observed to have smaller crystallite domains and a more uniform surface. 8YSZ_P ceramics fabricated with

aerosol spray pyrolysis sintering via SPS were observed have uniform and consistent pattern of crystallite domains.

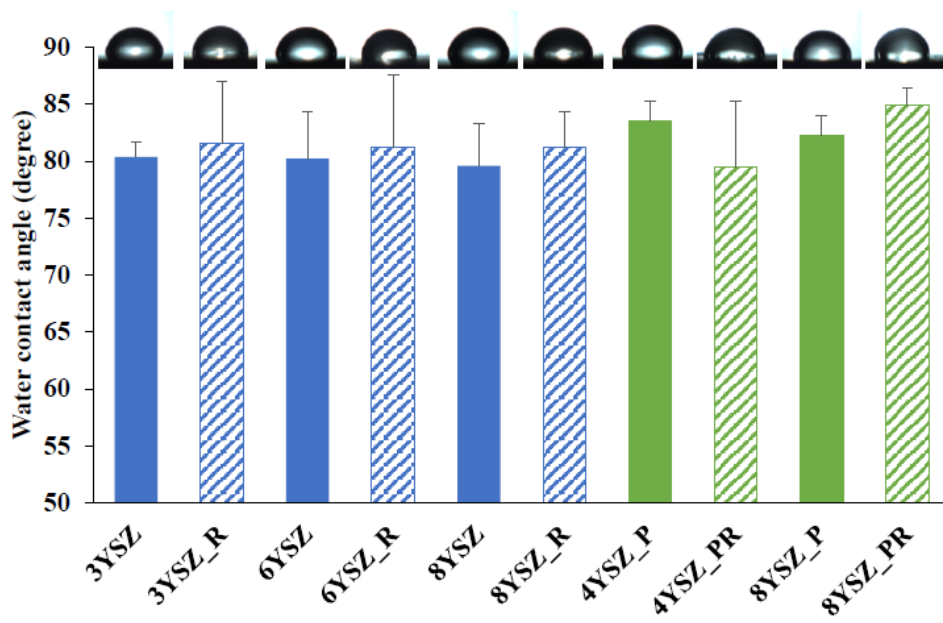


Figure 6. Water Contact Angle of YSZ samples

Figure 6 portrays the pictures of water droplet on the YSZ samples. All the YSZ samples were found to have less than 90 degree of contact angle. This indicates that polished and unpolished samples of different fabrication processes are all hydrophilic.

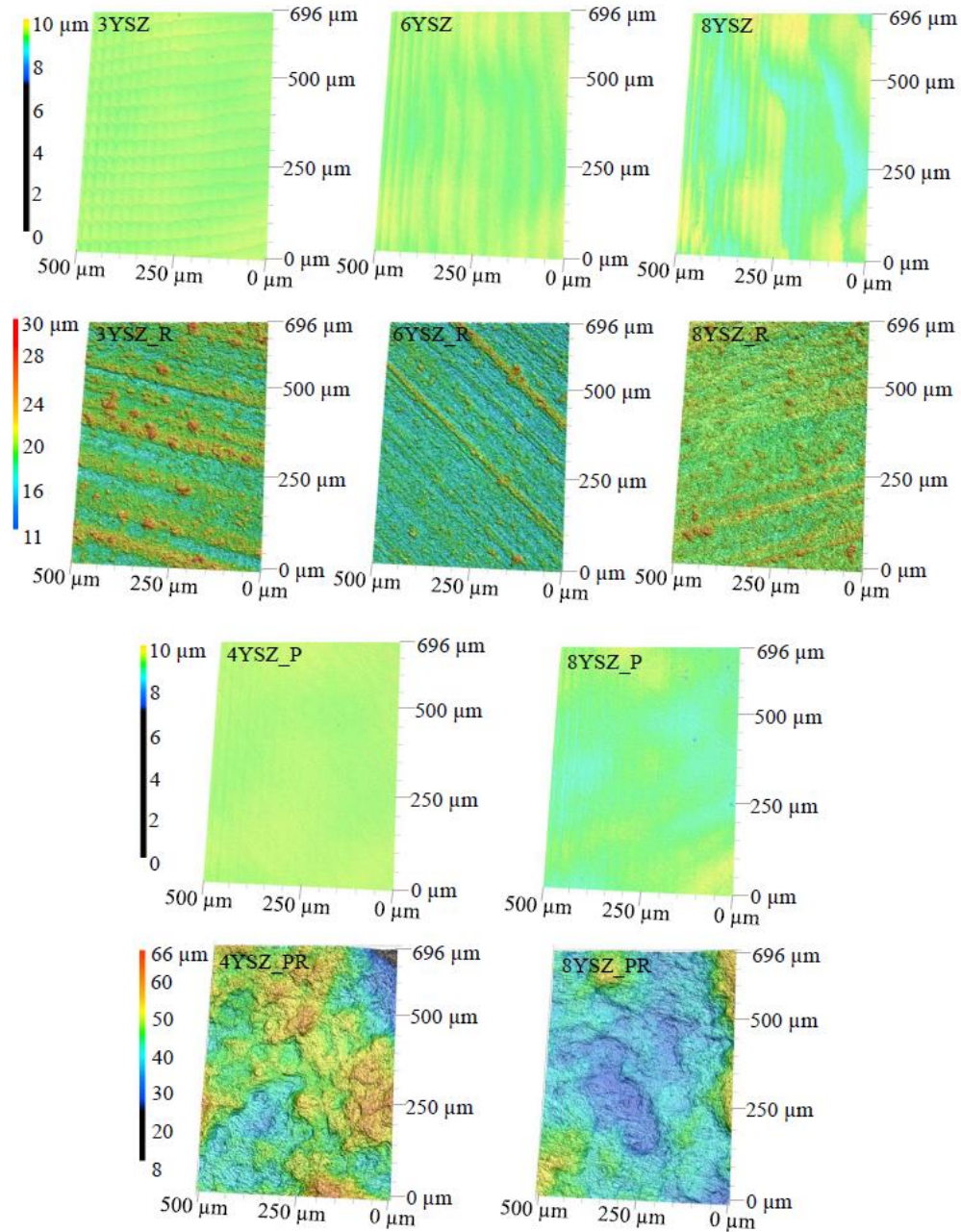


Figure 7. 3D microscopic images of YSZ ceramics

On Figure 7, the microscopic topographic images of polished and unpolished YSZ ceramics are shown. The polished YSZ ceramics have significantly less surface roughness than the unpolished samples, as shown by the color differences. All the polished samples portrayed a similar surface morphology. Unlike the unpolished samples, 3YSZ_R, 6YSZ_R, and 8YSZ_R

have similar crystalline pattern, which look like separated hills on flat land. The unpolished 4YSZ_PR and 8YSZ_PR ceramics also portrayed a cluster of mountains topography. This result also showed different fabrication method have different surface morphology.

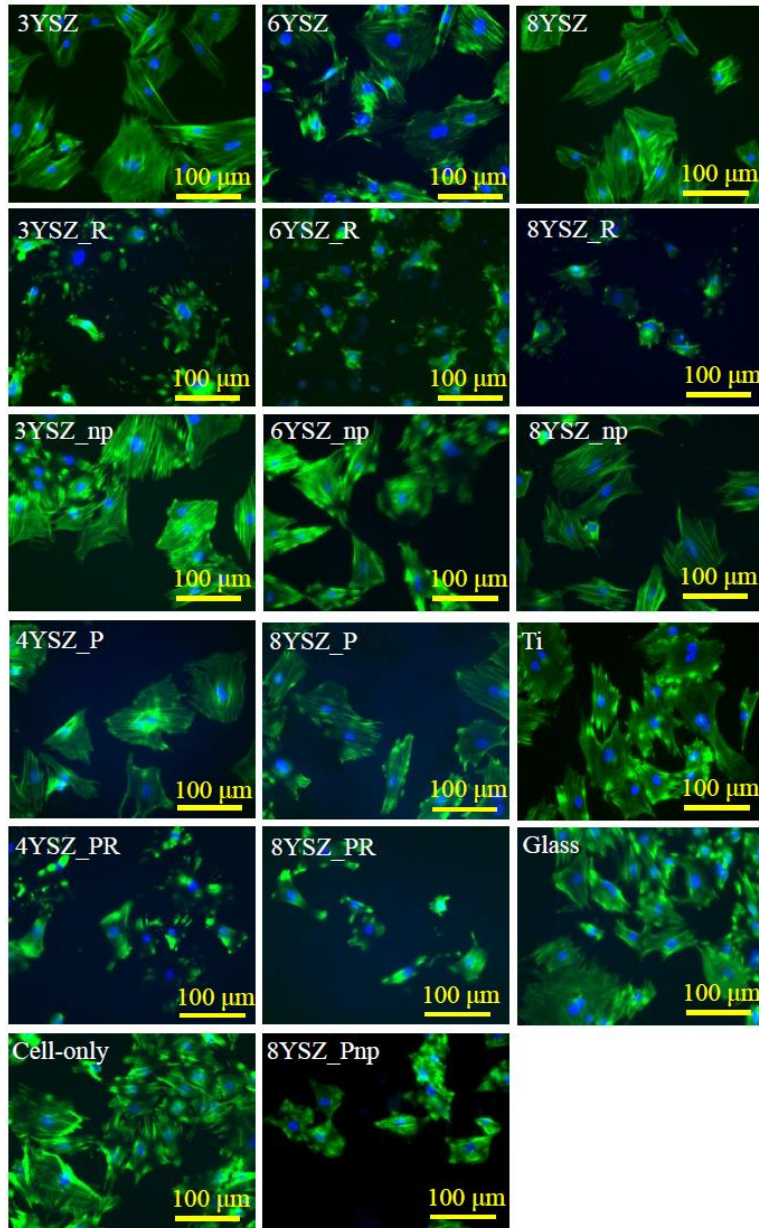


Figure 8. Cell behavior of direct culturing on YSZ ceramics

Figure 8 displays the fluorescent images of BMSCs after 24 hours of direct culturing on YSZ ceramics. Alexa Fluor 488-phalloidin stains the BMSCs' cytoskeleton structure to a bright

green-fluorescent color and DAPI stains the nucleus to a blue color. The cell spreading area, aspect ratio, and the number of cells were calculated by ImageJ software. The figure showed that the BMSCs have larger spreading area and rounder cytoskeleton on polished YSZ ceramics, while comparing to the unpolished counterpart. This confirmed our hypothesis that the BMSCs will not adhere and spread on the YSZ ceramics as well as the polished samples because the surface roughness impeded the available room for BMSCs to stretch.

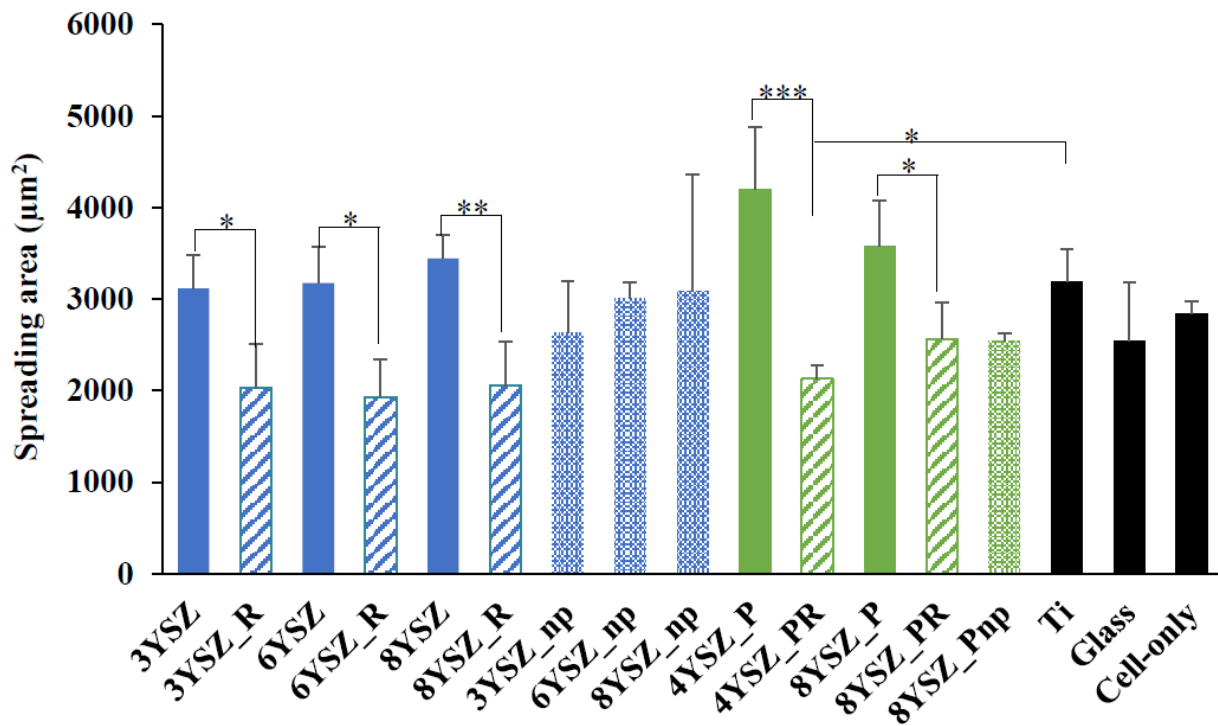


Figure 9. Average BMSCs spreading area of Each YSZ samples

Figure 9 portrays a bar graph of direct culturing BMSCs spreading area on different samples of YSZ ceramics calculating by ImageJ software and Excel. From the figure, all the polished samples have significantly greater spreading area than counterparts. There is no significant correlation between the concentration of yttria and the BMSCs spreading area. In addition, 3YSZ, 6YSZ, 8YSZ, 4YSZ_P, and 8YSZ_P have larger spreading area than the titanium and

glass control groups This indicated that the BMSCs grew better on these YSZ ceramic samples.

These calculated data also matched the observation in Figure 6.

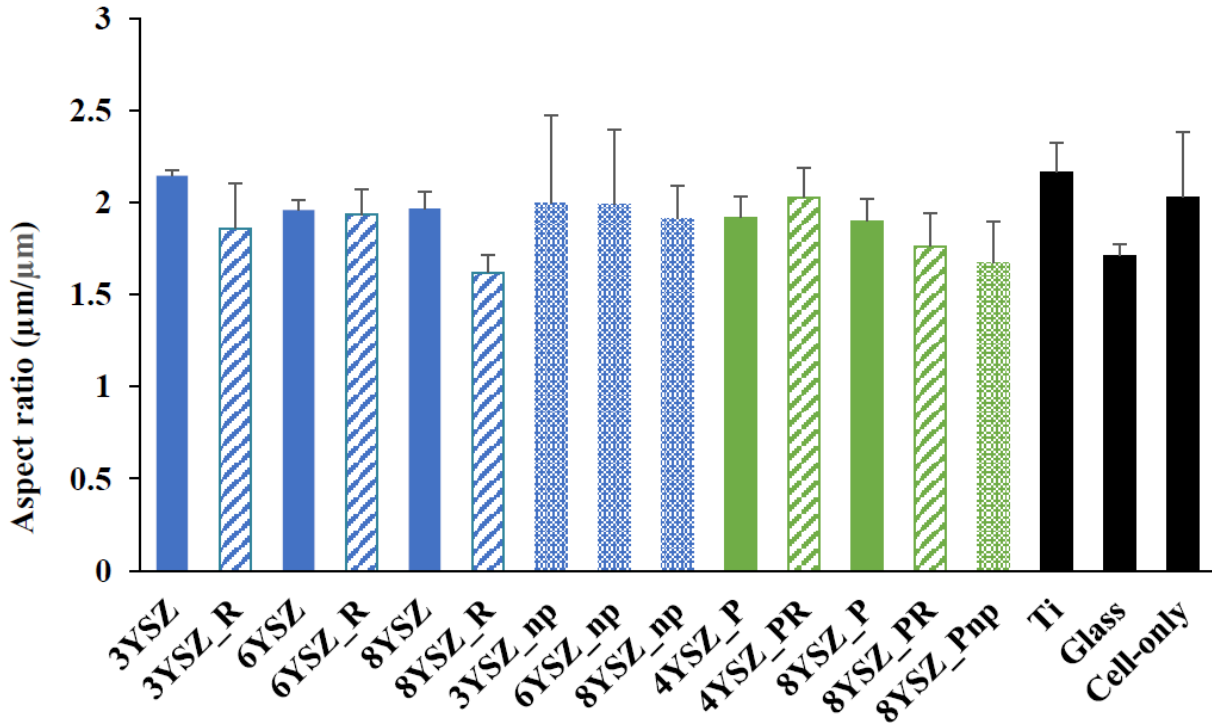


Figure 10. Average BMSCs Aspect Ratio of Each YSZ samples

Figure 10 also portrays a bar graph of direct culturing BMSCs aspect ratio on different samples of YSZ ceramics calculating by ImageJ software and Excel. Oppose to the observation on Figure 9, there are no significant differences between the polished and the unpolished counter parts. This demonstrates that the surface roughness, concentration of yttria, and the different methods of fabrication do not affect the aspect ratio of BMSCs. In addition, BMSCs seeded on the ceramic samples were found to have similar aspect ratio as the cell-only group, further indicating that the cytocompatibility of YSZ ceramics is great.

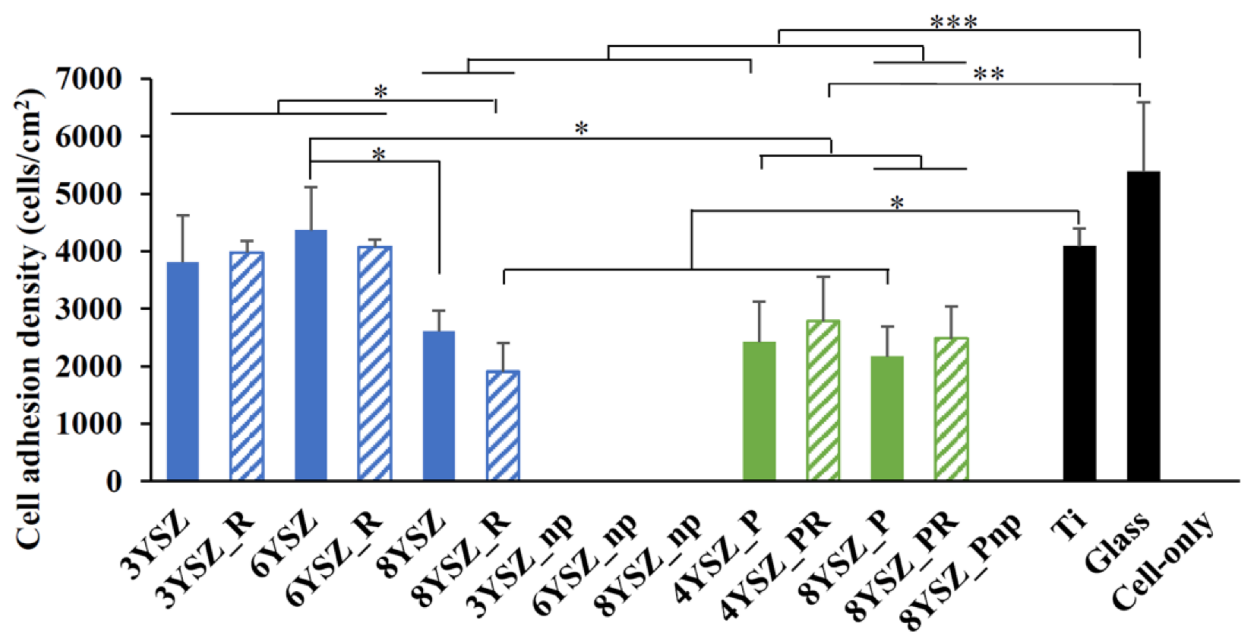


Figure 11. BMSCs Adhesion Density of Each YSZ samples

Figure 11 displays the BMSCs adhesion density of direct culturing on each different YSZ samples. The lines attached to the bar represent the standard deviations, and the lines above the bars represent the significant statistic differences between each sample. From the graph, there are no distinguish correlation between the polished and their unpolished counter parts, and all the YSZ samples were observed to have lower adhesion density than the glass control. The concentration of yttria does not significantly influence the cell adhesion density, either. However, the pyrolysis sintering YSZ ceramics reported to have lower cell adhesion density than the commercial nanoparticle sintering samples.

4. Discussion

YSZ ceramics are promising materials for window to the brain applications. The mechanical toughness, biocompatibility, and transparency established YSZ ceramics' capability. In this research, surface modifications, cell spreading areas, cell aspect ratio, and cell adhesion density have been studied. Because of optical transparency and accessibility, only the polished

YSZ samples will suffice for the window to the brain applications. As shown in Figure 5, a higher concentration of yttria in the same fabrication method, the finer and smaller the crystallite domains and polycrystalline grains. In addition, the YSZ ceramics fabricated via commercial nanoparticles sintering showed an irregular pattern of crystallite domains, but YSZ ceramics fabricated via aerosol spray pyrolysis sintering showed a more uniform crystallite pattern. However, another problem arises. A high concentration of yttria will result in a higher release of yttria to the surrounding tissues. Even though the release is very minimal, and the ceramic material are resisted to degradation, the toxicity of released yttria should be studied in future research. A longer culturing time can be performed in the future since the BMSCs were harvested 24hours in this research. In addition to optical transparency, YSZ ceramics fabricated via spray pyrolysis sintering with spark plasma sintering showed a lower cell adhesion density than commercial nanoparticles with ceramic sintering. Having a lower cell adhesion density, less cells will attach to the YSZ ceramics which leads to a better optical accessibility while performing laser therapy. Because, this will not only benefit the accuracy while performing laser therapy, but also eliminate the need of cleaning the attached cells for better views. Even though the YSZ samples have different surface morphology as shown in Figure 4, all the YSZ samples are hydrophilic. The water contact angles for all YSZ samples are less than 90 degrees as shown in Figure 6. This advantage will enhance the interaction between the YSZ and brain tissues. Figure 9 supports our hypothesis that unpolished counterparts will have smaller BMSCs spreading areas because the rough surface modification will impede the growth of each BMSC. Whereas in polished samples, there are barely any “walls” or “hills” will impede the stretch of each BMSC. There is no significance difference between the surface roughness and the BMSCs aspect ratio as shown in Figure 8. This also supports our hypothesis because the YSZ had

reported to have great biocompatibility. Therefore, concluding all the properties, we predicted that BMSCs adhesion density does not influence by the surface roughness but the surface morphology and the crystal structure. A best combination of optical transparency while maintaining the least adhesion density can be achieved in future studies.

5. Conclusion

In this study, we experimented the surface morphology, surface roughness, and surface hydrophilicity by fabricating the YSZ ceramics via commercial nanoparticles sintering, aerosol spray pyrolysis sintering, ceramic sintering, and spark plasma sintering. For each fabrication process, 3%, 6%, and 8% concentration of yttria to zirconia were also fabricated respectively. All the YSZ samples are hydrophilic regardless to the concentration nor the fabrication method. A higher concentration of yttria, the finer and smaller the crystallite domains and polycrystalline grains are. There is no significant difference of aspect ratio for each YSZ samples. The spreading area of BMSCs is much higher for polished samples than the unpolished counterparts. YSZ samples fabricated via spark plasma sintering and spray pyrolysis sintering showed the lowest cell adhesion density. This research will support YSZ ceramics as a strong candidate for the window to the brain application in terms of the cytocompatibility of BMSCs under direct culturing method.

6. Reference

- [1] Kazi, Gulsan Ara Sathi, and Ryo Yamagiwa. “Cytotoxicity and biocompatibility of high mol% yttria containing zirconia.” *Restorative dentistry & endodontics* vol. 45,4 e52. 14 Oct. 2020, doi:10.5395/rde.2020.45.e52
- [2] Salehpour, F., Mahmoudi, J., Kamari, F. *et al.* Brain Photobiomodulation Therapy: a Narrative Review. *Mol Neurobiol* **55**, 6601–6636 (2018). <https://doi.org/10.1007/s12035-017-0852-4>
- [3] Jean Geringer, Bernard Forest, Pierre Combrade, Fretting-corrosion of materials used as orthopaedic implants, *Wear*, Volume 259, Issues 7–12, 2005, Pages 943-951, ISSN 0043-1648,
- [4] M.J. Dalby, L. Di Silvio, E.J. Harper, W. Bonfield, Increasing hydroxyapatite incorporation into poly(methylmethacrylate) cement increases osteoblast adhesion and response, *Biomaterials*,
- [5] Muller, P.J. and Wilson, B.C. (2006), Photodynamic therapy of brain tumors—A work in progress. *Lasers Surg. Med.*, 38: 384-389. <https://doi.org/10.1002/lsm.20338>
- [6] Sai-Cheung Lee, Chieh-Tsai Wu, Shih-Tseng Lee, Po-Jen Chen, Cranioplasty using polymethyl methacrylate prostheses, *Journal of Clinical Neuroscience*, Volume 16, Issue 1, 2009, Pages 56-63, ISSN 0967-5868,
- [7] D. J. Bonda, BA, S. Manjila, MD, D. Dean, PhD. The Recent Revolution in the Design and Manufacture of Cranial Implants: Modern Advancements and Future Directions. *Neurosurgery*. Author manuscript; available in PMC 2016 November 01.
- [8] Lu, J.X., Huang, Z.W., Tropiano, P. *et al.* Human biological reactions at the interface between bone tissue and polymethylmethacrylate cement. *Journal of Materials Science: Materials in Medicine* 13, 803–809 (2002). <https://doi.org/10.1023/A:1016135410934>

[9] Zaza, Amin, Mohamed Habib, and Nabil Fatahalla. “Properties of PMMA Bone Cement Modified with Nano-Hydroxyapatite and Acetone.” *The Academic Research Community*

[10] C.I. Vallo, P.E. Montemartini, M.A. Fanovich, J.M. Porto López, T.R. Cuadrado Polymethylmethacrylate-based bone cement modified with hydroxyapatite

J Biomed Mater Res B, 48 (2) (2015), pp. 150-158

[11] Haas SS, Brauer GM, Dickson G. A characterization of polymethylmethacrylate bone cement. J Bone Joint Surg Am. 1975 Apr;57(3) 380-391. PMID: 1123392.

[12] Zaza, Amin, Mohamed Habib, and Nabil Fatahalla. “Properties of PMMA Bone Cement Modified with Nano-Hydroxyapatite and Acetone.” *The Academic Research Community publication 2.4* (2019): 489. *The Academic Research Community publication. Web.*

[13] Heini, P., Wälchli, B. & Berlemann, U. Percutaneous transpedicular vertebroplasty with PMMA: operative technique and early results . *E Spine J* 9, 445–450 (2000).

[14] Rutherford D, Exarhos S, Xu C, Niaccaris M, Mariano C, Dayap B, Mangolini L, Liu H. Synthesis, characterization, and cytocompatibility of yttria stabilized zirconia nanopowders for creating a window to the brain. J Biomed Mater Res B Appl Biomater. 2020 Apr;108(3):925-938. doi: 10.1002/jbm.b.34445. Epub 2019 Jul 24. PMID: 31339630.

<https://pubmed.ncbi.nlm.nih.gov/31339630/>

Table 1. YSZ disc groups and nanoparticle control groups for cell study

Polished	Unpolished	Nanoparticles
3YSZ	3YSZ_R	3YSZ_np
6YSZ	6YSZ_R	6YSZ_np
8YSZ	8YSZ_R	8YSZ_np
4YSZ_P	4YSZ_PR	4YSZ_Pnp
8YSZ_P	8YSZ_PR	8YSZ_Pnp

3, 6, 8 – Concentration of Ytria

P – Pyrolysis sintering

R – Rough

np – nanoparticles



prepared using commercial nanoparticle and fabricated via ceramic sintering

prepared using pyrolysis synthesized and fabricated via spark plasma sintering